LOAN DOCUMENT

PHOTOGRAPH THIS SHEET

AD-A276 458

DTIC ACCESSION NUMBER

LEVEL

1

INVENTORY

ARCSL-CR-82016

DOCUMENT IDENTIFICATION

Jun 82

DISTRIBUTION STATEMENT A

Approved for public release
Distribution Unlimited

DISTRIBUTION STATEMENT

NTIS	GRA&I
DTIC	TRAC
UNANNOUNCED	
JUSTIFICATION	
BY	
DISTRIBUTION/	
AVAILABILITY CODES	
DISTRIBUTION	AVAILABILITY AND/OR SPECIAL
A-1	

DISTRIBUTION STAMP

DTIC
ELECTE
MAR 2 1994
S C D

DATE ACCESSIONED

DATE RETURNED

94-05863

94 2 23 112

DATE RECEIVED IN DTIC

REGISTERED OR CERTIFIED NUMBER

PHOTOGRAPH THIS SHEET AND RETURN TO DTIC-FDAC

DTIC FORM 70A JUN 94

DOCUMENT PROCESSING SHEET

PREVIOUS EDITIONS MAY BE USED UNTIL STOCK IS EXHAUSTED.

LOAN DOCUMENT

HANDLE WITH CARE

CHEMICAL SYSTEMS LABORATORY CONTRACTOR REPORT

ARCSL-CR-82016

EXTINCTION BY RANDOMLY ORIENTED, AXISYMMETRIC PARTICLES

by

Ru T. Wang
Donald W. Schuerman

June 1982

Space Astronomy Laboratory
University of Florida
1810 N. W. 6th Street
Gainesville, Florida 32601

US ARMY ARMAMENT RESEARCH AND DEVELOPMENT COMMAND
Chemical Systems Laboratory
Aberdeen Proving Ground, Maryland 21010

DISCLAIMER

The views, opinions, and/or findings contained in this report are those of the authors and should not be construed as an official Department of the Army position, policy, or decision unless so designated by other documents.

DISPOSITION

Destroy this report when it is no longer needed. Do not return it to the originator.

SECURITY CLASSIFICATION OF THIS PAGE (When Data Entered)

REPORT DOCUMENTATION PAGE		READ INSTRUCTIONS BEFORE COMPLETING FORM
1. REPORT NUMBER ARCSL-CR-82016	2. GOVT ACCESSION NO.	3. RECIPIENT'S CATALOG NUMBER
4. TITLE (and Subtitle) EXTINCTION BY RANDOMLY ORIENTED, AXISYMMETRIC PARTICLES		5. TYPE OF REPORT & PERIOD COVERED Final, January 28, 1981 through August 25, 1981 6. PERFORMING ORG. REPORT NUMBER
7. AUTHOR(s) Ru T. Wang Donald W. Schuerman		8. CONTRACT OR GRANT NUMBER(s) DAAK-11-81-M-0010
9. PERFORMING ORGANIZATION NAME AND ADDRESS Space Astronomy Laboratory University of Florida 1810 NW 6th Street Gainesville, FL 32601		10. PROGRAM ELEMENT, PROJECT, TASK AREA & WORK UNIT NUMBERS 1L161102A71A-D
11. CONTROLLING OFFICE NAME AND ADDRESS Commander/Director, Chemical Systems Laboratory Attn: DRDAR-CLJ-R Aberdeen Proving Ground, MD 21010		12. REPORT DATE June 1982 13. NUMBER OF PAGES 21
14. MONITORING AGENCY NAME & ADDRESS (if different from Controlling Office) Commander/Director, Chemical Systems Laboratory Attn: DRDAR-CLB-PS (Dr. E. Stuebing) Aberdeen Proving Ground, MD 21010		15. SECURITY CLASS. (of this report) UNCLASSIFIED 15a. DECLASSIFICATION/DOWNGRADING SCHEDULE N/A

16. DISTRIBUTION STATEMENT (of this Report)

Approved for public release; distribution unlimited.

17. DISTRIBUTION STATEMENT (of the abstract entered in Block 20, if different from Report)

18. SUPPLEMENTARY NOTES

This study was sponsored by the Army Smoke Research Program, Chemical Systems Laboratory, Aberdeen Proving Ground, MD

Contract Project Officer: Dr. E. Stuebing, DRDAR-CLB-PS, (301) 671-3089

19. KEY WORDS (Continue on reverse side if necessary and identify by block number)

Extinction
Nonspherical particulates

20. ABSTRACT (Continue on reverse side if necessary and identify by block number)

The extinction, averaged over random particle orientations, is presented for each of 49 axisymmetric particles. These 2:1 prolate and oblate spheroids, 4:1 cylinders and disks, and 4:1 prolate and oblate spheroids have a variety of refractive indexes (m). Most results are from direct microwave analog measurements. Some were calculated according to the spheroid theory of Asano and Yamamoto (1975). The 49 extinctions are compared with those calculated by Asano and Sato (1980) for spheroids with m = 1.33 and aspect ratios of 2:1, 3:1, and 5:1. Salient features of the composite graph C_{EXT}/G *vs.* phase-shift parameter are discussed, where G is the geometric cross section of a volume-equivalent sphere.

DD FORM 1 JAN 73 1473 EDITION OF 1 NOV 65 IS OBSOLETE

SECURITY CLASSIFICATION OF THIS PAGE (When Data Entered)

PREFACE

The work performed under Contract No. DAAK-11-81-M-0010 was authorized under Project No. 1L161102A71A, SA-D, Aerosol Obscuration Science. The work was performed from January through August 1981.

The use of trade names in this report does not constitute an official endorsement or approval of the use of such commercial hardware or software. This report may not be cited for purposes of advertisement.

ACKNOWLEDGMENTS

This work was funded by the U. S. Army Chemical Systems Laboratory and the U. S. Army Research Office.

TABLE OF CONTENTS

LIST OF TABLES

LIST OF FIGURES

EXTINCTION BY RANDOMLY ORIENTED, AXISYMMETRIC PARTICLES

INTRODUCTION

The only experimental technique that permits systematic studies of single-particle extinction is the microwave analog method. The particle analog, a microwave target, can be arbitrarily oriented with respect to the incident beam so that $\overline{C_{EXT}}$, the extinction cross section averaged over a distribution of particle orientations, can be obtained as the (weighted) arithmetic mean of C_{EXT}, the orientation dependent, single-particle extinction. In a previous paper (Wang and Greenberg, 1978), the orientation dependence of C_{EXT} for 25 spheroids of aspect ratio 2:1 was presented in the form of P,Q plots (defined in a later section). In this report, the average extinction efficiency, $\overline{Q_{EXT}} = \overline{C_{EXT}}/G$ (G = an appropriate geometric cross section), for each spheroid is evaluated for a *random* distribution of particle orientations. To increase this unique and fundamental data base, 24 similarly averaged extinction efficiencies recently obtained by Schuerman *et al.* (1981) are included in the present discussion. The additional results were obtained by the microwave method and by the spheroid theory of Asano and Yamamoto (1975). They correspond to eight 2:1 spheroids (measured results, two of them also computed), four 4:1 disks (measured), four 4:1 cylinders (measured) and eight 4:1 spheroids (computed). All particles have axial symmetry, which facilitates the evaluation of $\overline{C_{EXT}}$. The effects of particle size, and refractive index on $\overline{C_{EXT}}$ are best shown by plotting $\overline{Q_{EXT}}$ against the phase-shift parameter of each particle. These plots are compared to extinction curves from Mie theory and to recent theoretical results of Asano and Sato (1980).

DEFINITIONS OF EXTINCTION EFFICIENCY

There are a number of ways in which the extinction cross section can be normalized to define the "extinction efficiency." In most of our former publications, the circular geometric cross section perpendicular to the rotation axis of a particle was taken as the normalization area. This simple definition provides a clear transition to experimental results of cylindrical particles. As theoretical methods became available for more complex particles and for the taking of averages over particle orientation, two more size parameters, and

hence their normalized cross sections, were introduced (Greenberg *et al.*, 1961; Wang *et al.*, 1977; Wang and Greenberg, 1978; Asano and Sato, 1980). They are the volume-equivalent size parameter $x_V = 2\pi a_V/\lambda$ and the surface-area-equivalent size parameter $x_S = 2\pi a_S/\lambda$. The a_V and a_S are the radii of spheres having respectively the same volume and the same surface area as the nonspherical particle. The random average of the projected area of any convex particle is equal to 1/4 of its total surface area (van de Hulst, 1957), or equivalently, to the geometrical cross section $G_S(=\pi a_S^2)$ of the equal-surface-area sphere. G_S is often used for normalization, and the resulting $\overline{Q_{EXT}}$ is denoted by $\overline{Q_{EXT,S}}$. If instead, the geometric cross section G_V of the equal-volume sphere is used, it is denoted by $\overline{Q_{EXT,V}}$. These two extinction efficiencies are obviously related by:

$$G_S\overline{Q_{EXT,S}} = G_V\overline{Q_{EXT,V}} = \overline{C_{EXT}}. \qquad (1)$$

The often raised question, "what is the most appropriate size parameter to describe the extinction produced by an arbitrarily oriented, nonspherical particle?" will remain as the subject of future study. We simply present two ways (equation 1) of representing the effect of particle size on extinction and point out that, at least for the size/shape range investigated here, more straightforward yet interesting extinction pictures are visualized if one chooses G_V. This selection has the further advantage of well describing lossy particles in the Rayleigh region where the extinction is primarily proportional to the particle volume.

TARGET PARAMETERS

Table 1 shows the target parameters as well as the $\overline{Q_{EXT}}$'s for 33 spheroidal analog particles of aspect ratio 2:1. The first 15 microwave targets described in that list were molded out of expandable polystyrene. In the next 10, the polystyrene was mixed with 2.5% carbon dust to introduce absorption. The refractive indexes of these 25 particles resemble that of water or dirty ice in the optical spectrum. P,Q plots which display the subtle orientation dependence of extinction of these 25 particles were included in a former report (Wang and Greenberg, 1978) and provided the data base from which the Q_{EXT}'s were calculated. The last eight spheroids in table 1 were machined from an acrylic material (lucite) and have $m = 1.61 - i0.004$. They simulate silicate particles in

Table 1. Microwave Target Parameters and Extinction Efficiencies, Averaged Over Random Particle Orientations, for 2:1 Spheroids

$m = m' - im''$ = complex refractive index; b = semi-axis along the axis of rotation; a = semi-axis perpendicular to the rotation axis; $x = 2\pi a/\lambda$; $\lambda = 3.1835$ cm; $\rho = 2x(m'-1)$; $\overline{Q_{EXT}}$ = extinction efficiency averaged over random orientations. Quantities referring to the radius or geometric cross section of *equal-surface-area* and *equal-volume* spheres are suffixed by S and V, respectively.

m'	m''	a(cm)	b(cm)	x_S	ρ_S	$\overline{Q_{EXT,S}}$	x_V	ρ_V	$\overline{Q_{EXT,V}}$
1.109	≈0.003	1.480	2.960	3.819	0.833	0.44	3.680	0.802	0.47
1.109	≈0.003	1.899	3.798	4.900	1.068	0.62	4.722	1.029	0.67
1.108	≈0.003	3.080	6.160	7.947	1.717	1.32	7.659	1.654	1.42
1.110	≈0.003	4.092	8.184	10.559	2.323	1.95	10.175	2.239	2.10
1.111	≈0.003	4.500	9.000	11.611	2.578	2.18	11.190	2.484	2.35
1.264	≈0.005	1.362	2.724	3.514	1.856	1.19	3.387	1.788	1.28
1.266	≈0.005	1.888	3.776	4.872	2.592	2.28	4.695	2.498	2.45
1.270	≈0.005	2.228	4.456	5.749	3.104	2.76	5.540	2.992	2.98
1.269	≈0.005	3.020	6.040	7.793	4.192	3.20	7.510	4.040	3.44
1.263	≈0.005	4.092	8.184	10.559	5.554	3.49	10.175	5.352	3.75
1.361	≈0.005	1.558	3.176	4.098	2.958	2.64	3.949	2.851	2.84
1.371	≈0.005	1.914	3.828	4.939	3.665	3.39	4.759	3.532	3.66
1.374	≈0.005	2.007	4.014	5.179	3.874	3.55	4.991	3.733	3.82
1.372	≈0.005	2.111	4.222	5.447	4.053	3.53	5.249	3.906	3.80
1.370	≈0.005	2.230	4.460	5.754	4.258	3.37	5.545	4.104	3.63

Continued on Next Page. . .

Table 1. Microwave Target Parameters and Extinction Efficiencies, Averaged Over Random Particle Orientations, for 2:1 Spheroids
(Continued, Page 2 of 2)

m'	m"	a(cm)	b(cm)	x_S	ρ_S	$\overline{Q_{EXT,S}}$	x_V	ρ_V	$\overline{Q_{EXT,V}}$
1.33	≈0.05	1.161	2.322	2.996	1.98	2.13	2.887	1.90	2.30
1.33	≈0.05	1.473	2.946	3.801	2.51	2.60	3.663	2.42	2.80
1.33	≈0.05	2.352	4.704	6.069	4.00	3.22	5.849	3.86	3.46
1.33	≈0.05	3.026	6.052	7.808	5.15	2.98	7.525	4.97	3.21
1.33	≈0.05	3.389	6.778	8.745	5.77	2.77	8.427	5.56	2.98
1.33	≈0.05	1.803	0.901	2.956	1.95	1.99	2.824	1.86	2.18
1.33	≈0.05	2.983	1.492	4.891	3.23	2.94	4.673	3.08	3.22
1.33	≈0.05	3.376	1.688	5.535	3.65	2.94	5.289	3.49	3.22
1.33	≈0.05	4.175	2.088	6.845	4.52	2.94	6.540	4.32	3.23
1.33	≈0.05	5.780	2.890	9.477	6.26	2.67	9.054	5.98	2.92
1.610	≈0.004	1.270	2.540	3.278	3.999	3.98	3.159	3.854	4.28
1.610	≈0.004	1.586	3.172	4.093	4.993	3.979*	3.944	4.812	4.268*
1.610	≈0.004	2.012	4.024	5.191	6.333	3.23	5.002	6.102	3.48
1.610	≈0.004	2.335	4.670	6.026	7.352	2.676*	5.807	7.084	2.882*
1.610	≈0.004	2.011	1.005	3.297	4.022	3.66	3.151	3.844	4.01
1.610	≈0.004	2.427	1.214	3.980	4.856	3.61	3.803	4.640	3.95
1.610	≈0.004	2.986	1.493	4.895	5.972	3.17	4.677	5.706	3.47
1.610	≈0.004	3.765	1.883	6.174	7.532	2.68	5.899	7.197	2.94

*Computed value from the sphroid theory of Asano and Yamamoto, *Appl. Opt.* 14, 29 (1975).

Table 2. Target Parameters and Extinction Efficiencies, Averaged Over Random Particle Orientations, for Axisymmetric Particles of Aspect Ratio 4:1

a = semi-axis perpendicular to the axis of rotation; b = semi-axis or ½ length along the rotation axis; $x = 2\pi a/\lambda$; λ = 3.1835 cm; $m = m' - im''$ = complex refractive index = 1.61 - i0.004 for all particles; $\rho = 2x(m'-1)$; $\overline{Q_{EXT}}$ = extinction efficiency averaged over random orientations — three significant figures for experimental values and four for theoretical. Quantities referring to the radius or geometric cross section of *equal-surface-area* and *equal-volume* spheres are suffixed by S and V, respectively.

Description	a(cm)	b(cm)	x_S	ρ_S	$Q_{EXT,S}$	x_V	ρ_V	$Q_{EXT,V}$
Cylinder	0.785	3.141	3.288	4.011	2.71	2.816	3.436	3.69
Cylinder	0.964	3.856	4.036	4.924	3.09	3.457	4.218	4.21
Cylinder	1.204	4.818	5.043	6.152	3.80	4.320	5.270	5.18
Cylinder	1.457	5.828	6.100	7.442	3.67	5.225	6.374	5.00
Prolate Spheroid	0.928	3.712	3.288	4.011	2.817	2.907	3.546	3.604
Prolate Spheroid	1.139	4.556	4.036	4.924	3.356	3.568	4.353	4.294
Prolate Spheroid	1.423	5.693	5.043	6.152	3.811	4.459	5.440	4.875
Prolate Spheroid	1.722	6.887	6.100	7.442	3.649	5.394	6.581	4.667
Oblate Spheroid	2.213	0.553	3.288	4.011	2.385	2.752	3.357	3.404
Oblate Spheroid	2.717	0.679	4.036	4.924	2.721	3.378	4.121	3.884
Oblate Spheroid	3.394	0.849	5.043	6.152	2.732	4.220	5.148	3.902
Oblate Spheroid	4.106	1.026	6.100	7.442	2.944	5.105	6.228	4.203
Disk	1.924	0.481	3.288	4.011	2.47	2.738	3.340	3.56
Disk	2.361	0.590	4.036	4.924	2.89	3.360	4.099	4.17
Disk	2.950	0.738	5.043	6.152	2.76	4.199	5.123	3.98
Disk	3.569	0.892	6.100	7.442	2.39	5.080	6.198	3.45

the optical region. Their extinction efficiencies were recently measured or, in the two cases denoted by asterisks, computed by Schuerman *et al.* (1981).

The averaged extinction efficiencies for 16 additional axisymmetric particles are listed in table 2, together with their target parameters. These four cylinders, four disks, four prolate spheroids, and four oblate spheroids have the same aspect ratio (4:1) and the same index of refraction ($1.61 - i0.004$). The cylinder and disk data are the microwave results; the spheroid data are from theoretical computations (Schuerman *et al.*, 1981). These particles were added to include more elongated/flattened particles, as well as to increase the range of the phase shift parameter (ρ_V). These 16 particles correspond to the range $3.3 \leq \rho_V < 6.6$ compared to $0.8 < \rho_V < 6.0$ for the 2:1 particles. In the latter group, the higher ρ_V values are sparsely populated.

AVERAGING THE θ=0 SCATTERING QUANTITIES OVER RANDOM PARTICLE ORIENTATIONS

$\overline{C_{EXT}}$ is a simple average of orientation-dependent extinctions, but measuring the single-particle extinction for each member of a large sample of particle orientations is a time consuming enterprise. For particles with an axis of symmetry, an equivalent average can be obtained in a much simplified manner (Wang and Greenberg, 1978). The symmetry axis needs only be swept through 90° from the incident $\vec{k}_0$ direction in two mutually orthogonal planes, the k-E plane and and the k-H plane, that contain the $\vec{k}_0,\vec{E}_0$ and the $\vec{k}_0,\vec{H}_0$ vectors of the incident wave, respectively (see figure 1). At any other arbitrary particle orientation (χ, ψ), where χ is the tilt angle of the axis from $\vec{k}_0$ and ψ is the azimuth angle around $\vec{k}_0$, all matrix elements of the θ=0 complex scattering amplitude (van de Hulst, 1957) are linear compositions of those obtained in these two orthogonal planes (Wang, 1968):

$$
\begin{aligned}
S_1(\chi,\psi) &= S_R^E(\chi)\cos^2\psi + S_R^H(\chi)\sin^2\psi + i\left[S_I^E(\chi)\cos^2\psi + S_I^H(\chi)\sin^2\psi\right], \\
S_2(\chi,\psi) &= S_R^E(\chi)\sin^2\psi + S_R^H(\chi)\cos^2\psi + i\left[S_I^E(\chi)\sin^2\psi + S_I^H(\chi)\cos^2\psi\right], \qquad (2) \\
S_3(\chi,\psi) &= S_4(\chi,\psi) = \left[S_R^H(\chi) - S_R^E(\chi)\right]\cos\psi\sin\psi + i\left[S_I^H(\chi) - S_I^E(\chi)\right]\cos\psi\sin\psi,
\end{aligned}
$$

where $S_R^E(\chi)$ and $S_I^E(\chi)$ are respectively the real and imaginary part of the complex, θ=0 scattering amplitude when the symmetry axis is in the k-E plane, tilted by χ from $\vec{k}_o$; $S_R^H(\chi)$ and $S_I^H(\chi)$ are those in the k-H plane.

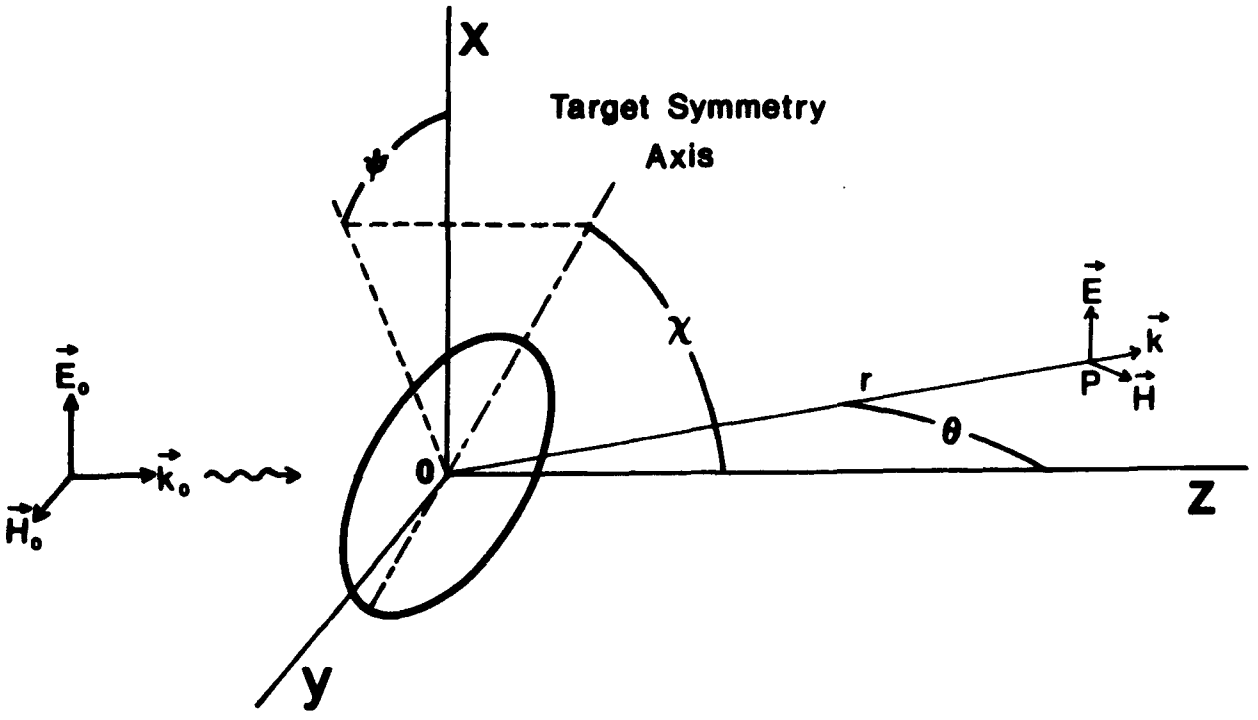

Figure 1. Target-Orientation Angles (χ, ψ), Scattering Angle (θ), and the Geometry of Scattering.

The extinction cross section $C_{EXT}(\chi, \psi)$ at each orientation follows from equations (2) and the Optical Theorem:

$$C_{EXT} = \frac{4\pi}{k^2} \text{Re}\left\{S_1(\chi,\psi)\right\} = \frac{4\pi}{k^2}\left[S_R^E(\chi)\cos^2\psi + S_R^H(\chi)\sin^2\psi\right]$$
$$= C_{EXT}^E(\chi)\cos^2\psi + C_{EXT}^H(\chi)\sin^2\psi \quad . \tag{3}$$

Here again superscripts E and H denote whether the symmetry axis is in the k-E or k-H plane. $\overline{C_{EXT}}$, the average of $C_{EXT}(\chi,\psi)$, is then obtained as

$$\overline{C_{EXT}} = \frac{1}{4\pi}\int_0^{\pi}\sin\chi d\chi \int_0^{2\pi} C_{EXT}(\chi,\psi)d\psi = \frac{1}{2}\int_0^{\frac{\pi}{2}}\left[C_{EXT}^E(\chi)+C_{EXT}^H(\chi)\right]\sin\chi d\chi \quad . \tag{4}$$

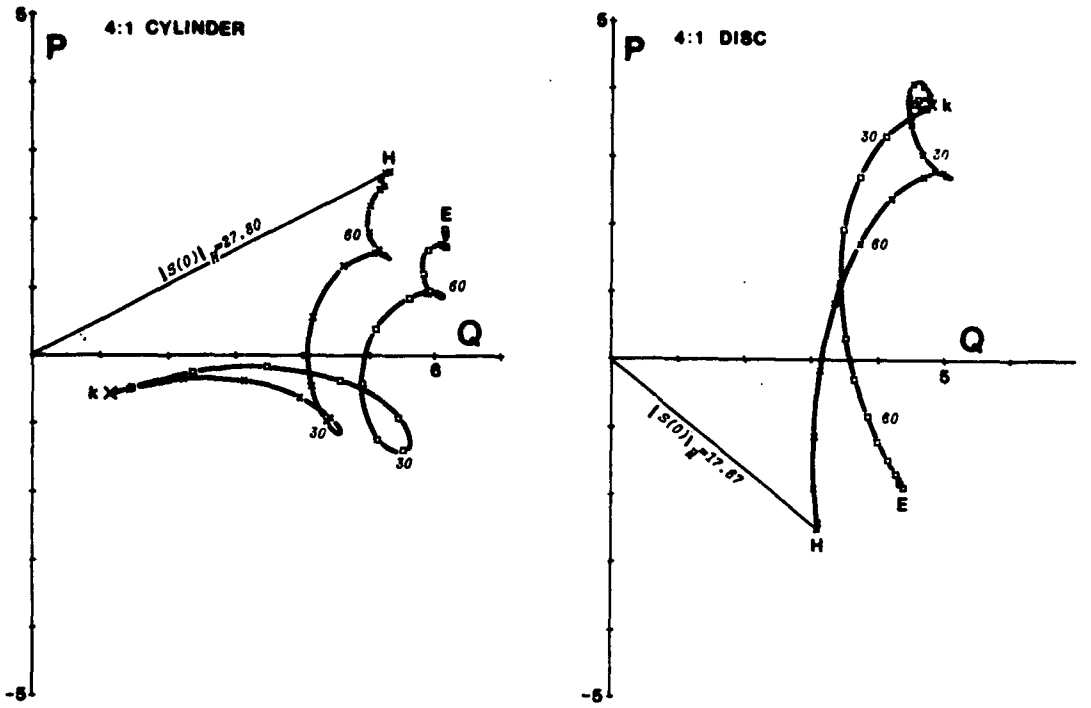

Figures 2A and 2B. P,Q Plots of a 4:1 Circular Cylinder (A) and 4:1 Circular Disk (B).

The two P,Q plots display the target orientation dependence (χ, in deg.) of the complex forward-scattering amplitude S(0) for two axially symmetric particles. The two curves in each plot are generated by sweeping the particle axis through 90^o from the incident direction $\vec{k}_o(\chi=0^o)$ toward the $\vec{E}_o$ and $\vec{H}_o$ directions in two orthogonal planes, the k-E and the k-H plane of the incident wave, respectively. A vector drawn from the coordinate origin to any point along the curve gives S(0) at that particle orientation, while the projection of the same vector onto the calibrated Q-axis yields the extinction efficiency $Q_{EXT,V} = C_{EXT}/\pi a_V^2$. The magnitude of the forward-scattering amplitude, $|S(0)|$, at any orientation can be determined by comparing the length of its vector to that of $S(0)_H = S(\frac{\pi}{2},\frac{\pi}{2})$ whose magnitude is shown in each graph. The target parameters and the average extinction efficiencies are respectively: (figure 2A) $x_V = ka_V = 4.320$, $m = 1.61\text{-}i0.004$, $\overline{Q_{EXT,V}} = 5.18$; (figure 2B) $x_V = ka_V = 4.199$, $m = 1.61\text{-}i0.004$, $\overline{Q_{EXT,V}} = 3.98$.

Two P,Q plots, obtained by the microwave technique, are shown in figures 2A and 2B. They respectively refer to the third cylinder and the third disk listed in table 2. Each P,Q plot is a cartesian recording of the complex forward scattering amplitude $S(\chi, \psi)$ as a function of particle orientation. The particle axis is swept from the incident $\vec{k}_0$ direction (χ=0) to the incident $\vec{E}_0$ or $\vec{H}_0$ directions (χ=π/2) in the k-E plane (ψ=0) and in the k-H plane (ψ=π/2) to generate the double curve in each figure. A vector drawn from the coordinate origin to any point on the curves represents $S_1(\chi,0 \text{ or } \pi/2)$. Its absolute magnitude can be found by comparing the length of this vector with that of $|S(0)|_H = |S_1(\frac{\pi}{2},\frac{\pi}{2})|$ shown in each figure. The tilt of the S_1 vector from the P-axis is the phase-shift $\phi(0)$ of the θ=0 scattered wave at this particle orientation, and the projection of this vector onto the Q-axis gives the extinction efficiency. Both the P and Q axes are calibrated in units of $\overline{Q_{EXT,V}}$ for the particle under investigation. (see also Wang, 1980)

The numerical integration over χ for the evaluation of the random average is accomplished by Simpson's rule with $\Delta\chi = 5^\circ$ in all experimental cases. The P,Q plots for cylinders and disks contain curves rich in loops and cusps, but it is our experience that 5° increments in χ produce errors which are small compared to other experimental errors. Most of the older spheroid data, obtained before the target orientation process was automated (Schuerman *et al.*, 1981), were taken with $\Delta\chi = 10^\circ$ ($\Delta\chi = 30^\circ$ for very small particles). The larger increments were mandated by the slower, manual operation of target orientating; the data had to be obtained before susceptible null-drift (Wang, 1968) occurred. In such cases, the missing C_{EXT} data points were filled in by a third order Aitken-Lagrange interpolation technique (Todd, 1967).

RESULTS AND DISCUSSION

It is impossible to combine the three factors of size, shape, and index of refraction into a single, independent variable that uniquely describes the full range of resonant extinction phenomena. This impossibility prevails even when the shape factor is degenerate, as in the case of spheres. Nevertheless, the use of a single independent variable is a useful, though approximate, method of describing salient features of the extinction curve. The first to define such a variable — the phase-shift parameter $\rho_V = 2x_V(m-1)$ — was van de Hulst (1946, 1957) in his anomalous diffraction theory of extinction. The undeviated but phase-shifted rays passing through the particle form a modified wave-front

in the shadow of the particle which interferes with the incident ray to produce resonance phenomena in extinction. The quantity ρ_V is the phase shift suffered by the diametrically transmitted ray with respect to the unperturbed incident ray. This approximation theory is known to predict the general futures of $Q_{EXT,V}$ *vs.* ρ_V curves. The approximation does yield some errors: (a) all spheres possessing the same ρ_V have identical $Q_{EXT,V}$, (b) there are no minor ripples in the extinction curve, (c) the value of Q_{EXT} may have an error of up to 30% near the resonance peaks, and (d) the shift in peak extinction is underestimated as the particle absorption increases. While these numerical deficiencies can now be easily removed by employing rigorous Mie solutions instead of the original approximation formula, the essential physics of the extinction phenomena is still governed by the single parameter, ρ_V. Its use has been extended to cases of nonspheres on numerous occasions (Greenberg, 1960, 1968; Greenberg, *et al.*, 1961, 1963, 1967, 1971; Wang 1980), and that practice will be continued here.

The dependence of $\overline{Q_{EXT,V}}$ on ρ_V for the 49 axisymmetric particles listed in tables 1 and 2 is plotted in figure 3. Different symbols are used to identify 11 distinct refractive-index and target-shape groups. A number of conspicuous features appear on this plot:

(1) Randomly-oriented, axisymmetric particles do exhibit resonance extinction with respect to variations in ρ_V, with the largest m = 1.27, 2:1 prolate spheroid being the sole exception.

(2) The first major resonance is noticeably broadened. For spheroids, the greater the aspect ratio, the broader the peak; sufficient data do not yet exist to test this trend for other shapes.

(3) For the 2:1 spheroids, the magnitude and location of the resonance are not much different from those predicted by Mie theory for spheres possessing the same refractive index if the minor ripples for the latter are ignored. The prolate peak is somewhat higher and shifted toward higher ρ_V.

(4) Beyond the first major resonance, all particles obscure the incident light more efficiently than *spheres* of the same ρ_V, a feature also observed for rough particles (Wang, 1980).

(5) Beyond the first major resonance for spheres, the extinction is strongly dependent on the aspect ratio as well as on shape. The greater the aspect ratio, the larger the $\overline{Q_{EXT,V}}$ and the larger is

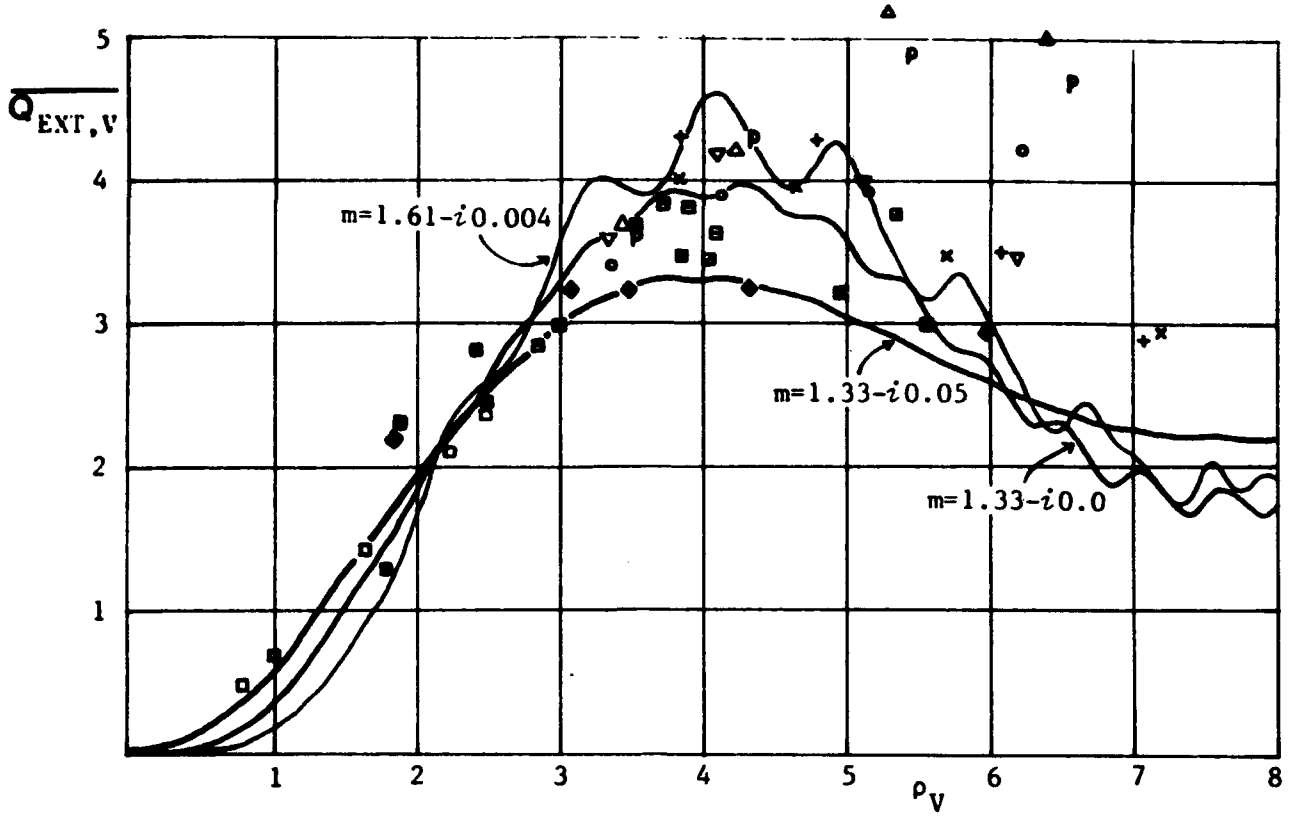

Figure 3. $\overline{Q_{EXT,V}}$ *vs.* ρ_V Plots for 49 Axisymmetric Particles.

2:1 spheroids with low refractive indexes
- □ m≈1.11-i0.003 prolate spheroids
- ▨ m≈1.27-i0.005 prolate spheroids
- ▣ m≈1.37-i0.005 prolate spheroids
- ■ m≈1.33-i0.05 prolate spheroids
- ◆ m≈1.33-i0.05 oblate spheroids

The continuous curves are for spheres.

Particles with m = 1.61-i0.004 (silicate like)
- ▲ 4:1 cylinders
- p 4:1 prolate spheroids
- ✚ 2:1 prolate spheroids
- x 2:1 oblate spheroids
- o 4:1 oblate spheroids
- ▼ 4:1 disks

the ρ_V at which the extinction peaks. It is curious that the 4:1 oblate spheroids produce a shoulder in extinction near $\rho_V \simeq 4.5$ which is absent for the 4:1 disks.

(6) For 4:1 particles, prolates (elongated particles) dim the incident light more efficiently than oblates (flattened particles) beyond the resonance in the range $3.5 \lesssim \rho_V \lesssim 6.3$.

(7) From $\rho_V \simeq 4$ to $\rho_V = 0$, the difference in extinction due to shape gradually diminishes and the particle's volume becomes the most significant factor in extinction.

(8) The 2:1 prolate spheroids with m = 1.11 - i0.003 have the smallest ρ_V for their given sizes. These particles behave like absorbing spheres with m = 1.33 - i0.05, a phenomenon also observed for rough particles of similar refractive index (Wang, 1980).

(9) Although some uncertainties in the refractive index (m = 1.33 - i0.05) of the small-sized 2:1 spheroids can result in errors in their ρ_V scale of up to $\Delta\rho_V \approx 0.3$, these small, absorbing spheroids seem to behave also like absorbing spheres of higher Re{m} and Im{m}.

Meanwhile, theoretical results on scattering by randomly oriented spheroidal particles of various aspect ratios have been published by Asano and Sato (1980). They plotted $\overline{Q_{EXT,V}}$ *vs.* x_V for water-like spheroids, m = 1.33 - i0.0, with aspect ratios of 1:1, 2:1, 3:1, and 5:1. Their results for oblate (figure 4A) and prolate (figure 4B) spheroids were cast in the same format as our figure 3 by our reading of numerical values from their graphs, converting their x_V's into ρ_V's, and plotting their results on a similar scale. A continuous curve for a single sphere and a discrete plot for size-dispersed (Hansen-Travis distribution; see references in Asano and Sato, 1980) spheres have been added to both figures 4A and 4B. Those spheres have m = 1.33 - i0.0. The overlaying of figure 4A and/or 4B on figure 3 permits a comparison between the theory and experiment. The above mentioned features (1) through (7) in figure 3 are also present in figure 4A-4B, notwithstanding the absence of 4:1 spheroids in the latter. The magnitudes and positions of extinction peaks agree in form with those in figure 3 including the shoulder at $\rho_V \approx 4.5$ for 5:1 oblate spheroids. The numerical differences in magnitude are due to detailed differences in refractive index, shape, and size. Ripples, a characteristic of spherical particles or smooth particles in fixed orientation, are not present in these extinction curves even though pronounced ripples may appear for particles of higher aspect ratios or refractive indexes (Barber *et al.*, 1982).

SUMMARY

Tentative conclusions derived from this research are:

(1) Extinction by nonspherical particles is best discussed in terms of their volume-equivalent phase-shift parameters, ρ_V.

(2) Randomly oriented, axisymmetric particles distinctly differ from spheres in their extinction when $\rho_V \gtrsim 4$ (i.e., beyond the first

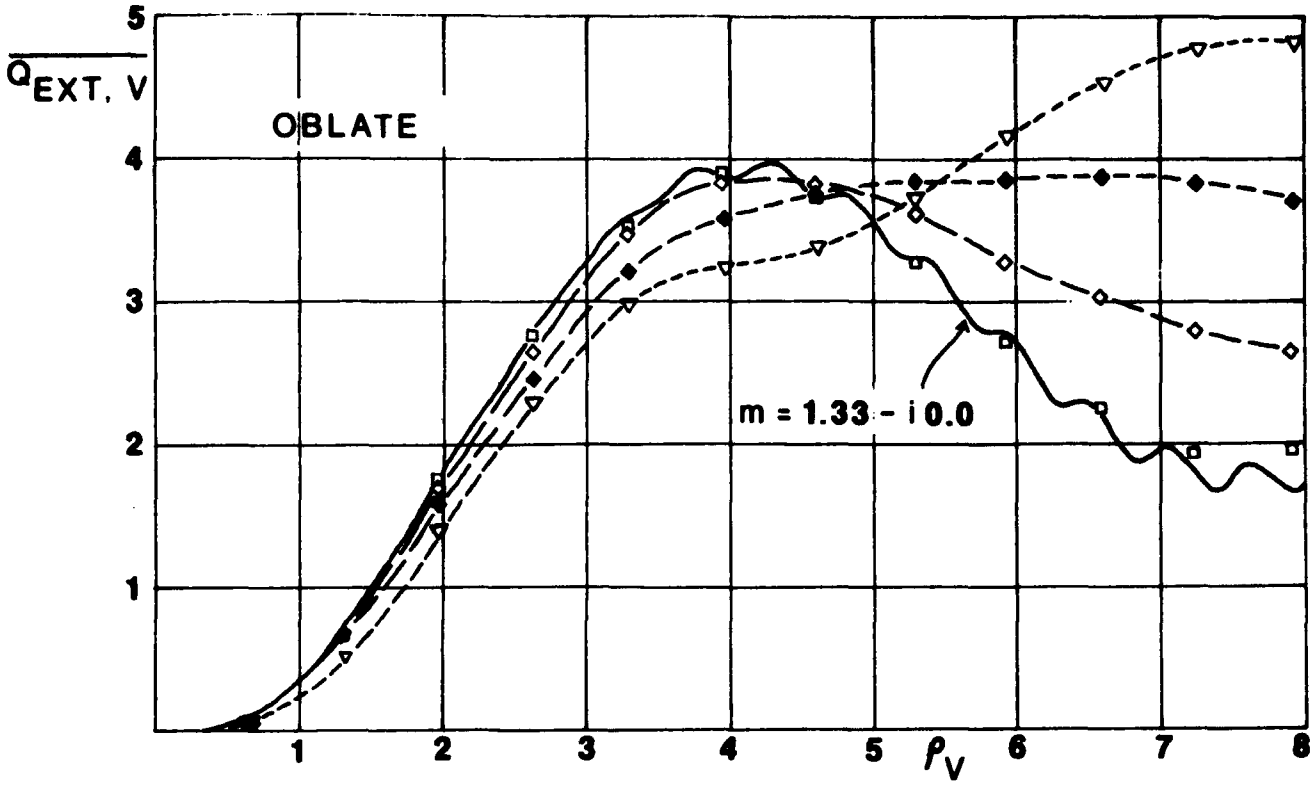

Figure 4A. Theoretical Extinction Curves for Randomly Oriented Oblate Spheroids. The spheroids have a common index of refraction (1.33-i0.0). Their aspect ratios of 5:1, 3:1 and 2:1 are indicated by the number of slashes between data points. For example, ▽-----▽ indicates results for 5:1 oblate spheroids, ◇--◇ for 2:1 oblate spheroids, etc. These $\overline{Q_{EXT,V}}$ *vs.* ρ_V plots were constructed from graphs by Asano and Sato (*Appl. Opt.* 19, 962, 1980) in order to compare with the results shown in Figure 3 on the same scale. Continuous curve represents the extinction by spheres; the unconnected □ symbols represent size-dispersed spheres (Hansen-Travis distribution used by Asano and Sato. See the article cited above).

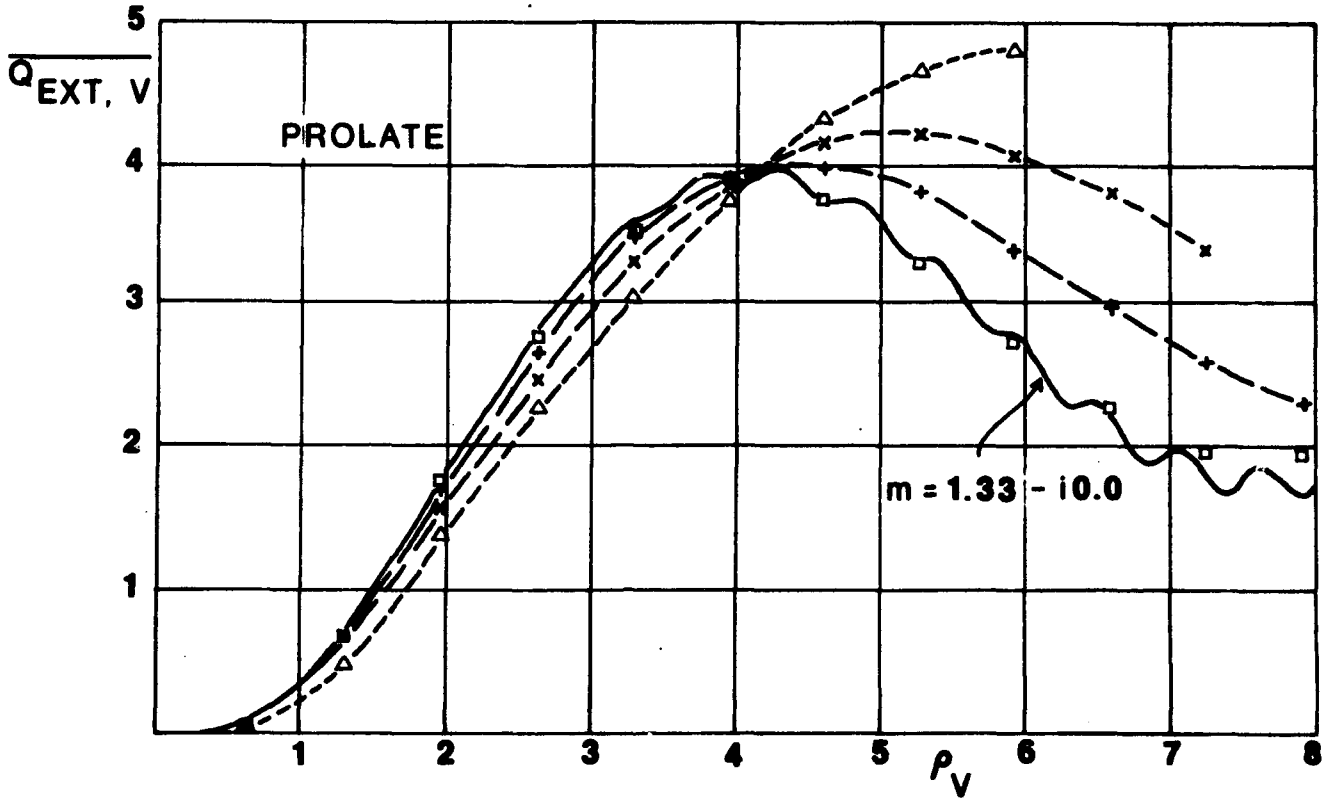

Figure 4B. Theoretical Extinction Curves for Randomly Oriented Prolate Spheroids.

Same as Figure 4A except that all spheroids here refer to prolates.

resonance) and have higher extinction efficiencies per unit volume than spheres.

(3) For $3 \lesssim \rho_V \lesssim 6$, elongated particles produce more extinction per unit volume than do flattened ones if both have the same aspect ratio and refractive index.

(4) Noticeable differences in extinction exist between equally flattened disks and oblate spheroids; and, in a less conspicuous way, between a cylinder and a prolate spheroid of the same elongation.

(5) From $\rho_V \lesssim 4$ to $\rho_V = 0$, the effect of shape gradually diminishes as the particle volume becomes the dominant factor in extinction.

(6) For $\rho_V \lesssim 1.5$, low-absorbing nonspheres behave like spheres with higher absorption.

Although the number of nonspheres in this report is quite limited, lacking those particles of very large aspect ratio and unusually high refractive indexes, their extinction may crudely represent that produced by many naturally occurring particulates.

REFERENCES

Asano, S. and G. Yamamoto, *Appl. Opt.* 14, 29, 1975.

Asano, S. and M. Sato, *Appl. Opt.* 19, 962, 1980.

Barber, P. W., J. F. Owen, and R. K. Chang, *IEEE Trans. Ant. Prop. AP-30*, 168, 1982.

Greenberg, J. M., *J. Appl. Phys.* 31, 82, 1960.

_____, in "Nebulae and Interstellar Matter," B. M. Middlehurst, and L. H. Aller, eds., Univ. of Chicago Press, p. 221, 1968.

Greenberg, J. M., N. E. Pedersen, and J. C. Pedersen, *J. Appl. Phys.* 32, 233, 1961.

Greenberg, J. M., A. C. Lind, R. T. Wang, and L. F. Libelo, in "Electromagnetic Scattering," M. Kerker, ed., Pergamon, New York, p. 123, 1963.

_____, in "Electromagnetic Scattering," L. Rowell and R. Stein, eds., Gordon and Breach, New York, p. 3, 1967.

Greenberg, J. M., R. T. Wang, and L. Bangs, *Nature, Phys. Sci.* 230, 110, 1971.

Schuerman, D. W., R. T. Wang, B. Å. S. Gustafson, and R. W. Schaefer, *Appl. Opt.* 20, 4039, 1981.

Todd, J., in "Handbook of Phys.," E. U. Condon and H. Odishaw, eds., McGraw Hill, New York, p. 1-94, 1967.

van de Hulst, H. C., "Thesis Utrecht," Recherches, Astron. Obs. d'Utrecht, 11, Part I, 1946.

_____, in "Light Scattering by Small Particles," John Wiley & Sons, New York, 1957.

Wang, R. T., Ph.D. thesis, Rensselaer Polytechnic Institute, Troy, New York, 1968.

_____, in "Light Scattering by Irregularly Shaped Particles," D. W. Schuerman, ed., Plenum Press, New York, p. 255, 1980.

Wang, R. T. and J. M. Greenberg, Final Report, NASA NSG 7353, August 1978.

Want, R. T., R. W. Detenbeck, F. Giovane and J. M. Greenberg, Final Report, NSF ATM75-15663, June 1977.

DISTRIBUTION LIST

Addressee	Copies
Defense Technical Information Center ATTN: DTIC-DDA-2 Cameron Station, Building 5 Alexandria, VA 22314	2
Director U.S. Army Material Systems Analysis Activity ATTN: DRXSY-MP Aberdeen Proving Ground, MD 21005	1
Commander U.S. Army Armament Research & Development Command ATTN: DRDAR-TSS Dover, NJ 07801	2
Commander/Director Chemical Systems Laboratory	
ATTN: DRDAR-CLB-	1
ATTN: DRDAR-CLB-A (Record Set)	1
ATTN: DRDAR-CLB-P	1
ATTN: DRDAR-CLB-PS	10
ATTN: DRDAR-CLN-S	2
ATTN: DRDAR-CLJ-L	2
ATTN: DRDAR-CLJ-R	2
ATTN: DRDAR-CLJ-M	1
ATTN: DRDAR-CLY-A	1
ATTN: DRDAR-CLY-R	1
Aberdeen Proving Ground, MD 21010	
Commander USA ARRCOM ATTN: SARTE Aberdeen Proving Ground, MD 21010	1
Project Manager Smoke/Obscurants ATTN: DRCPM-SMK Aberdeen Proving Ground, MD 21005	2